

Calculation of Nonperturbative Terms in Open String Models

Julie D. Blum

Physics Department
University of Texas at Austin
Austin, TX 78712 USA

Abstract

Nonperturbative corrections in type II string theory corresponding to Riemann surfaces with one boundary are calculated in several noncompact geometries of desingularized orbifolds. One of these models has a complicated phase structure which is explored. A general condition for integrality of the numerical invariants is discussed.

1. Introduction

String theory has provided mathematicians with many interesting conjectural results that would be in some cases significantly more difficult to obtain through traditional techniques. Calculations that count the number of maps from Riemann surfaces into Calabi-Yau manifolds are one example. Recently, these calculations have been extended to Riemann surfaces with boundaries. The addition of boundaries for a generic type II string theory reduces the supersymmetry to $N = 1$ in four dimensions, and the counting of maps corresponds to holomorphic terms in the field theory. Such calculations are possibly relevant to an extension of the Standard Model.

In the following we will calculate the nonperturbative terms in a type II string theory generated by Riemann surfaces with one boundary, “disk instantons”. Most of the techniques that will be employed here are discussed in [1], [2], and other places. In honor of human decency, no additional references will be mentioned. We will focus on three noncompact models, the blowups of the $\mathbf{Z}_2 \times \mathbf{Z}_2$, $\mathbf{Z}_2 \times \mathbf{Z}_4$, and \mathbf{Z}_7 orbifolds of \mathbf{C}^3 . The three models support the conjecture that numerical invariants related mathematically to the Euler characteristic of the moduli space of open string instantons and physically to the counting of domain walls are integral in phases where Kahler parameters have a geometric interpretation. The second model has an intricate moduli space with many phases. We explore the phase structure of this model and see how it reduces in various limits to simpler models. The complications of this model necessitated an understanding of what conditions ensure integrality of the numerical invariants. We explain why the geometric phases always give integers and the conditions under which fractions are possible.

2. $\mathbf{Z}_2 \times \mathbf{Z}_2$

2.1. Toric Geometry

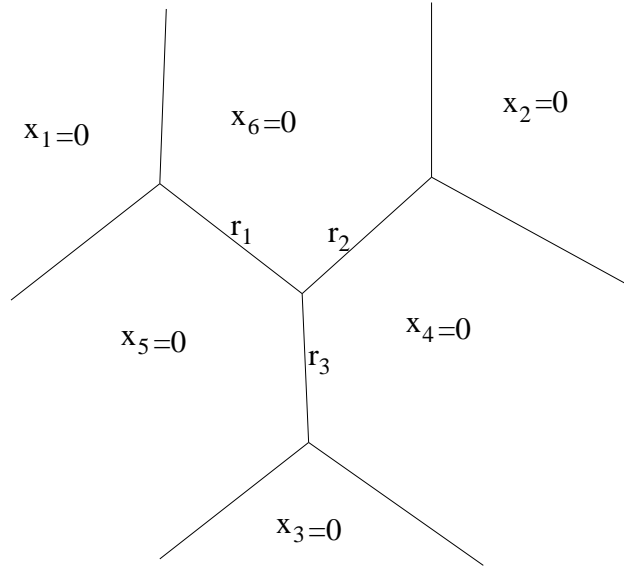
The toric geometry for this model can be described by a linear sigma model (two dimensional abelian gauge theory with $N = 2$ supersymmetry). There are six chiral fields carrying the following charges under three $U(1)$ gauge fields.

$$\begin{aligned} l_1 &= (1, 0, 0, 1, -1, -1) \\ l_2 &= (0, 1, 0, -1, 1, -1) \\ l_3 &= (0, 0, 1, -1, -1, 1) \end{aligned} \tag{2.1}$$

The Calabi-Yau condition requires $\sum_j l_i^j = 0$. From the set of charges, one derives the D-terms in the gauge theory.

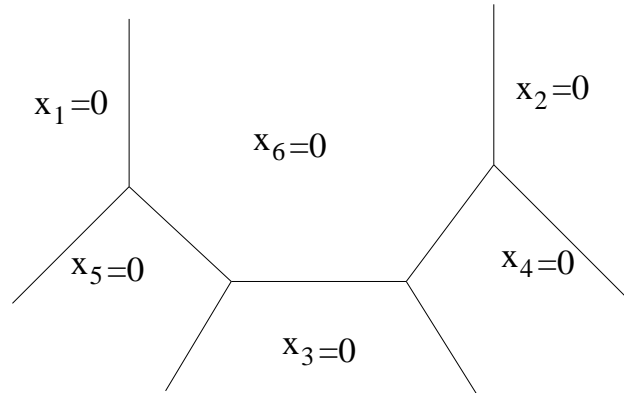
$$\sum_j l_i^j |x_j|^2 = r_i \quad (2.2)$$

These equations can be solved leading to the following “toric diagram”.



Diag. 1. Toric Diagram of $\mathbf{Z}_2 \times \mathbf{Z}_2$ Blowup

The diagram is a projection of three dimensions onto the plane, and the angles shown are not meant to be accurate. Generically, the diagram represents a \mathbf{T}^3 fibration. It shrinks to a two-torus along planes $x_i = 0$, to a circle along lines $x_i = x_j = 0$, and to a point at the intersection of three lines. From the diagram one sees that there are three two-spheres and six noncompact two-cycles. Since this diagram resembles the intersection of three conifolds, one would expect other phases that replace a \mathbf{P}^1 by an \mathbf{S}^3 . One can easily visualize a flopped phase as the following where $r_3 \rightarrow -r_3$.



Diag. 2. Toric Diagram of $\mathbf{Z}_2 \times \mathbf{Z}_2$ Flopped Phase: $r_3 \rightarrow -r_3$

The equation for the $\mathbf{Z}_2 \times \mathbf{Z}_2$ singularity can be obtained from gauge invariant combinations of chiral fields as $w^2 = xyz$ where w , x , y , and z are complex variables.

To show explicitly that there are three \mathbf{P}^1 's, one should solve the Picard-Fuchs equations. These equations determine the Kahler parameters for the \mathbf{P}^1 's corrected by world-sheet instantons or equivalently complex parameters in the local mirror geometry, i.e. $\int_{\gamma_i} \Omega$, where Ω is the holomorphic three-form and γ_i is a three-cycle. For this model the equations are

$$[\Theta_1(\Theta_1 - \Theta_2 - \Theta_3) - z_1(\Theta_1^2 - (\Theta_2 - \Theta_3)^2)] \int_{\gamma_i} \Omega = 0 \quad (2.3)$$

and cyclic permutations where $\Theta_i = z_i \partial_{z_i}$ and $z_i = e^{-t_i}$ with $t_i = r_i + i\theta_i$, the initial Kahler parameter. Here θ_i is a Fayet-Iliopoulos parameter in the linear sigma model. One takes linear combinations of the $\int_{\gamma_i} \Omega$ normalized appropriately to obtain \hat{t}_i , the instanton corrected Kahler parameters. For the calculation here we need the inverse solutions which turn out to be

$$z_1 = \frac{q_1(1 + q_2q_3)}{(1 + q_1q_2)(1 + q_1q_3)} \quad (2.4)$$

and permutations where $q_i = e^{-\hat{t}_i}$. Note that in finding unique solutions for the Picard-Fuchs equations, we have frequently had to change to a different basis of \mathbf{P}^1 's. The simplicity of these solutions makes this model amenable to obtaining exact results without great labor.

2.2. The Mirror and Open String Amplitudes

The equation for the mirror is readily derived from $Re(y_i) = -|x_i|^2$, the D-term equations, and $xz = \sum_i e^{y_i}$ where x and z are complex variables. Setting $y_5 = u$, $y_6 = v$, and $y_4 = 0$ to fix a constant solution of the D-term equations yields

$$xz = P(u, v) = 1 + e^u + e^v + e^{-t_1+u+v} + e^{-t_2+v-u} + e^{-t_3+u-v}. \quad (2.5)$$

A noncompact, supersymmetric Lagrangian three-cycle in the original manifold is determined by three additional constraints which in this case take the form

$$\begin{aligned} |x_5|^2 - |x_4|^2 &= c_1 \\ |x_6|^2 - |x_4|^2 &= c_2 \\ \sum_i Arg(x_i) &= 0 \text{ and/or } \pi. \end{aligned} \quad (2.6)$$

Let us write the above in the form

$$\sum_j l_p^{(1)j} |x_j|^2|_{3\text{-cycle}} = c_p \quad (2.7)$$

and

$$\sum_j l^{(2)i} \text{Im}(\log(x_i|_{3\text{-cycle}})) = 0 \text{ and/or } \pi \quad (2.8)$$

for later use. Here $\sum_i l_p^{(1)i} l^{(2)i} = 0$ makes the cycle Lagrangian and $\sum_i l_p^{(1)i} = 0$ is necessary for supersymmetry of the Lagrangian cycle. Additionally, $\sum_i l_j^i l^{(2)i} = 0$ implies that (2.8) is gauge invariant. If the cycle does not intersect a compact or noncompact two-cycle in the base, both $\sum_i \text{Arg}(x_i) = 0$ and $\sum_i \text{Arg}(x_i) = \pi$ are needed to give a composite cycle without boundary. For this case any worldsheet disks that intersect a D-brane wrapped on the two cycles will be oppositely oriented with respect to the two cycles and not make a contribution. If the cycle intersects the toric base, one can choose either $\sum_i \text{Arg}(x_i) = 0$ or $\sum_i \text{Arg}(x_i) = \pi$ to get a cycle without boundary, and there generally will be a nonvanishing contribution from disks wrapping part of a \mathbf{P}^1 and intersecting the cycle in a circle. Allowing the three-cycle to end on the \mathbf{P}^1 where $x_6 = x_4 = 0$ (which will be denoted as Phase I), the classical limit in the mirror corresponds to $v = i\pi$, $\text{Re}u = -c_1 \approx \frac{-r_2}{2} \rightarrow -\infty$, and $xz = 0$. More generally, one can choose the mirror two-cycle of the Lagrangian three-cycle to be parametrized by z with $x = P(u, v) = 0$, a Riemann surface which is the moduli space of this cycle. The coordinates u and v can be considered as transverse coordinates to a two-cycle inside a Calabi-Yau manifold.

The disk amplitude $\mathcal{F}_{g=0, h=1}$ (g is the genus, h is the number of boundaries) can be determined classically in the mirror as $\partial_u \mathcal{F}_{0,1} = v$ where classically $v = 0$ and u parametrizes the area of a disk. In the original manifold, these disks can be interpreted as domain walls (e.g. fourbranes wrapping a disk) ending on a sixbrane wrapped on the three-cycle. The tension of these domain walls is corrected by an amount δu that must be added to the classical area of a disk. The amplitude $\mathcal{F}_{0,1}$ takes the form

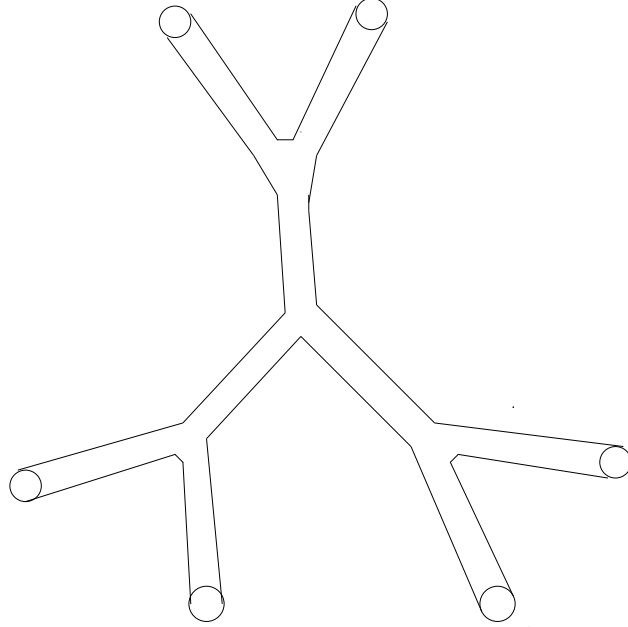
$$\mathcal{F}_{0,1} = \sum_{k,n,\vec{m}} \frac{1}{n^2} N_{k,\vec{m}} \left(\prod_i q_i^{m_i n} \right) e^{\hat{u}kn} \quad (2.9)$$

where k, n, m_i are integers, \hat{u} is the instanton corrected domain wall tension, and $N_{k,\vec{m}}$ counts the number of domain walls wrapping the two-cycle parametrized by $\sum_i m_i \hat{t}_i$ with a boundary wrapping the \mathbf{S}^1 k times. The assumption is that one counts isolated domain

walls and that the $N_{k,\bar{m}}$ should be integers. If one has a continuous family of domain walls, fractions may be possible. In section three we will determine a criterion for obtaining integers and present an argument for integrality in those cases. Under mirror symmetry a domain wall fourbrane becomes a domain wall fivebrane with tension determined classically by $\hat{u} = u - \delta u$ where $\delta u = \frac{1}{2\pi i} \int_{C_u} u dv$ and $v \rightarrow v + 2\pi i$ around the one-cycle on the Riemann surface C_u . This tension corresponds to the difference in the superpotential $\mathcal{F}_{0,1}$ as one crosses the domain wall. In the original manifold, the change in $\text{Im}v$ corresponded to the change in Wilson line as one crossed the domain wall.

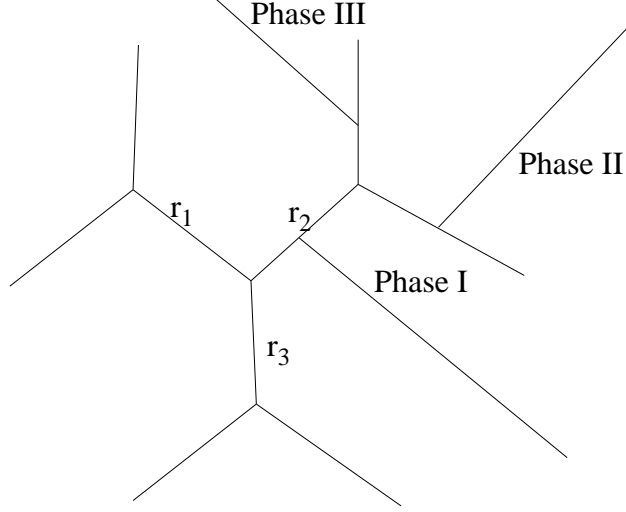
There is an ambiguity in $\mathcal{F}_{0,1}$ due to the possibility of redefining the disk coordinate $\hat{u} \rightarrow \hat{u} + n\hat{v}$ where n is an integer since $v = 0$ classically. One requires n to be an integer so that $e^{\hat{u}}$ is invariant under $\hat{u} \rightarrow \hat{u} + 2\pi i$. This ambiguity can sometimes be related to moving the Lagrangian cycle to a different phase along the toric base, and the amplitude $\mathcal{F}_{0,1}$ is not invariant. If the toric base is modeled by type IIB fivebranes, the ambiguity corresponds to an $SL(2, \mathbf{Z})$ transformation of type IIB.

Proceeding with the calculation, the Riemann surface $P(u, v) = 0$ looks like the following diagram where the legs extend to infinity.



Diag. 3. Riemann Surface $P(u, v) = 0$ in mirror of $\mathbf{Z}_2 \times \mathbf{Z}_2$ Blowup

There are nine phases, but the three compact \mathbf{P}^1 's and the six noncompact two-cycles of the original manifold are related by symmetries reducing the number of inequivalent phases to two.



Diag. 4. Phases for noncompact three-cycle in $\mathbf{Z}_2 \times \mathbf{Z}_2$ Blowup

For instance, the three inner phases are exchanged by exchanging $z_3 \leftrightarrow z_2 \leftrightarrow z_1$ along with $v \leftrightarrow u \leftrightarrow -u$, and phase II and phase III are exchanged under $z_1 \leftrightarrow z_3$, $v \leftrightarrow -v$. Phase II corresponds to $c_1 = c_2 + r_2$, $c_2 \gg 0$.

In phase I one obtains

$$v = i\pi - \ln 2(1 + z_1 e^u + z_2 e^{-u}) + \ln[(1 + e^u) + \sqrt{(1 + e^u)^2 - 4z_3(e^u + z_1 e^{2u} + z_2)}] \quad (2.10)$$

Extracting the piece of v that is independent of e^u gives δv , and one has

$$\delta v = \frac{t_1 - \hat{t}_1}{2} - \frac{t_3 - \hat{t}_3}{2} + i\pi. \quad (2.11)$$

To get δu , we exchange t_3 and t_2 so

$$\delta u = \frac{t_1 - \hat{t}_1}{2} - \frac{t_2 - \hat{t}_2}{2} + i\pi. \quad (2.12)$$

In the above equation for v , we must substitute, $v = \hat{v} + \delta v$, $u = \hat{u} + \delta u$, and $z_i(q_i)$. Note that not all of the classical symmetries of the superpotential are preserved by the corrections, and one cannot determine the correction uniquely by symmetry. The result is

$$\begin{aligned} \hat{v} = & -\ln(1 - q_1 e^{\hat{u}})(1 - q_2 e^{-\hat{u}}) \\ & - \sum'_{m,n,a,b,c,d,e} (-1)^{m+b+c} \frac{(2n+m-1)! e^{\hat{u}(2a+b+c)} q_1^{a+d+e} q_2^{m+n-a-b-c+d} q_3^{m+n-c+e}}{n! a!(c-e)! e!(b-d)!(m-c)! d!(n-a-b)!} \end{aligned} \quad (2.13)$$

The \sum' indicates that we omit terms independent of $e^{\hat{u}}$. Clearly the first term of \hat{v} has the required form. The lowest order terms of the second summation can be examined by hand or calculated on a computer using Mathematica, and one does obtain $N_{k,\vec{m}}$ that are integers after integrating and comparing with (2.9). One can show explicitly that all $N_{1,\vec{m}}$ are integers. One finds $N_{1,0,m,m} = -\sum_{n=1}^m \frac{(-1)^{n+m}(n+m-1)!m}{n!^2(m-n)!}$, $N_{1,1,m-1,m} = \sum_{n=0}^{m-1} \frac{(-1)^{n+m}(n+m-1)!}{n!^2(m-n-1)!}$, and $N_{1,0,m-1,m} = N_{1,1,m,m} = \sum_{n=1}^m \frac{(-1)^{n+m}(n+m-1)!}{n!(n-1)!(m-n)!}$. We have verified that all N_{k,m_1,m_2,m_3} are integers for $k \leq 10$, $m_1 \leq 1$, $m_2 \leq 1$, and $m_3 \leq 10$. Rather than present this data which is very cumbersome, we give three tables with k and m_3 set to specific values.

Table 1:

$$m_3 = 5, k = 5$$

m_2	$m_1=0$	1	2	3	4	5
0	5	-14	14	-6	1	0
1	-126	350	-350	150	-25	1
2	756	-2100	2100	-900	150	-6
3	-1764	4900	-4900	2100	-350	14
4	1764	-4900	4900	-2100	350	-14
5	-635	1764	-1764	756	-126	5

Table 2:

$$m_3 = 5, k = 6$$

m_2	$m_1=0$	1	2	3	4	5
0	42	-126	140	-70	15	-1
1	-630	1890	-2100	1050	-225	15
2	2940	8820	9800	-4900	1050	-70
3	-5880	17640	-19600	9800	-2100	140
4	5292	-15876	17640	-8820	1890	-126
5	-1764	5292	-5880	2940	-630	42

The diagonal symmetry $N_{k,m_1-x,m_2-y,m_1+m_2} = N_{k,m_1+y,m_2+x,m_1+m_2}$ is generated by $d \leftrightarrow b - d$ in (2.13). The similar symmetry $N_{k,m_1-x,m_1+m_3-k,m_3-y} = N_{k,m_1+y,m_1+m_3-k,m_3+x}$ is generated by $e \leftrightarrow c - e$.

Table 3:

$$m_3 = 5, k = 7$$

m_2	$m_1=0$	1	2	3	4	5
0	198	-630	756	-420	105	-9
1	-2310	7350	-8820	4900	-1225	105
2	9240	-29400	35280	-19600	4900	-420
3	-16632	52920	-63504	35280	-8820	756
4	13860	-44100	52920	-29400	7350	-630
5	-4356	13860	-16632	9240	-2310	198

In phase II we do the coordinate transformation $u \rightarrow u' = u - v + t_2$, $v \rightarrow v' = v$. Correspondingly, $\delta u' = \delta u - \delta v + \delta t_2 = \frac{t_3 - \hat{t}_3}{2} + \frac{t_2 - \hat{t}_2}{2}$ and $\delta v' = \delta v$. Phase II is almost equivalent to phase I. One obtains phase II from (2.13) by ignoring the first log term, exchanging $q_2 \leftrightarrow q_3$ and $\hat{u} \leftrightarrow \hat{v}$. The first term is similar to the inner phase of a conifold so it looks like the \mathbf{S}_3 symmetry relating the inner and two outer phases is broken by the finite \mathbf{P}^1 's.

One can extract amplitudes in the flopped phase of Diagram(2) by taking $q_3 \rightarrow q'_3 = 1/q'_3$, $q_1 \rightarrow q'_1 q'_3$, $q_2 \rightarrow q'_2 q'_3$, and $\exp \hat{u} \rightarrow q'_3 \exp \hat{u}'$ in (2.13). As a check on our results, the conifold in the two inequivalent phases is retrieved in the limit $q_1, q_3 \rightarrow 0$. Replacing the \mathbf{P}^1 by an \mathbf{S}^3 in this limit via a conifold transition also yields the same result from the calculation of the expectation value of a Wilson line in the Chern-Simons theory on \mathbf{S}^3 . It would be interesting to extend such calculations to the case of multiple \mathbf{S}^3 's.

3. $\mathbf{Z}_2 \times \mathbf{Z}_4$

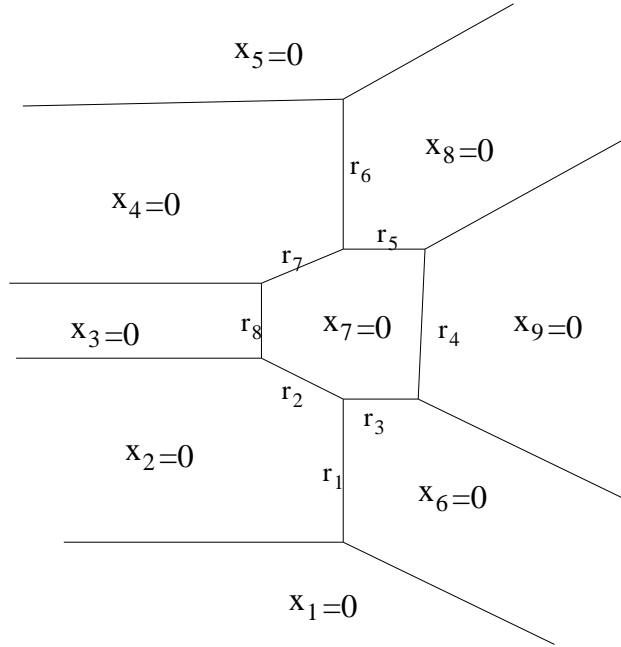
3.1. Toric Geometry

Let us move on to the $\mathbf{Z}_2 \times \mathbf{Z}_4$ case. Here we increase the complexity of the calculation, but the results reduce precisely to the $\mathbf{Z}_2 \times \mathbf{Z}_2$ case in a particular limit. We start with

the following set of charges under six $U(1)$'s for nine fields.

$$\begin{aligned}
l_1 &= (1, -1, 0, 0, 0, -1, 1, 0, 0) \\
l_2 &= (0, -1, 1, 0, 0, 1, -1, 0, 0) \\
l_3 &= (0, 1, 0, 0, 0, -1, -1, 0, 1) \\
l_4 &= (0, 0, 0, 0, 0, 1, -2, 1, 0) \\
l_5 &= (0, 0, 0, 1, 0, 0, -1, -1, 1) \\
l_6 &= (0, 0, 0, -1, 1, 0, 1, -1, 0)
\end{aligned} \tag{3.1}$$

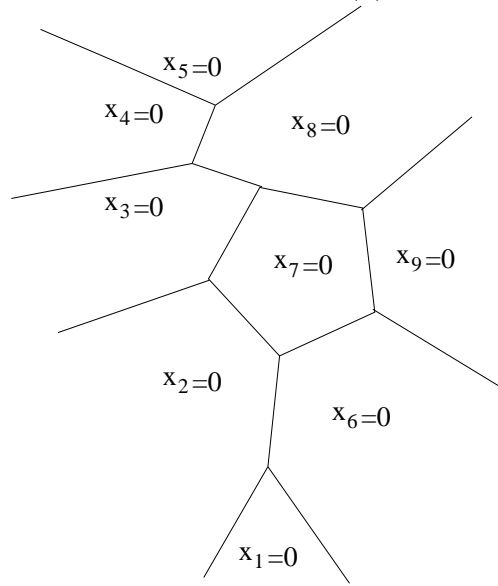
yielding $\sum_j l_i^j |x_j|^2 = r_i$. Solving these equations leads to the following toric diagram in one particular region of moduli space



Diag. 5. Toric Diagram of $\mathbf{Z}_2 \times \mathbf{Z}_4$ Blowup

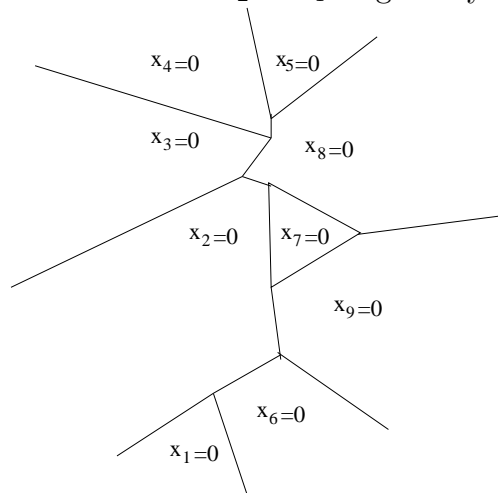
where $r_7 = r_2 + r_3 - r_5 > 0$, $r_8 = -2r_2 - r_3 + r_4 + r_5 > 0$, and all of the r_i are large. The four-cycle represented by the hexagon is a \mathbf{P}^2 blown up in succession at three points (one obtains inequivalent four-cycles depending on how one does this). It is also equivalent to the \mathbf{F}_2 Hirzebruch surface blown up at two points. By taking r_4 and r_8 to infinity, the above diagram and the theory reduces to two decoupled $\mathbf{Z}_2 \times \mathbf{Z}_2$ cases. There are possible flop transitions to other geometric phases for r_1, r_2, r_3, r_5, r_6 , and r_7 but not for r_4 and r_8 . Shrinking r_8 to a negative value removes a \mathbf{P}^1 as $|x_3| > 0$ everywhere, and we enter

a nongeometric phase where a Kahler parameter loses its correspondence to a geometric \mathbf{P}^1 . The result of flopping r_7 is shown in Diagram (6).



Diag. 6. Toric Diagram of $\mathbf{Z}_2 \times \mathbf{Z}_4$ Flopped Phase: $r_7 \rightarrow -r_7$

Two more flops ($r_4 - r_2 \rightarrow r_2 - r_4, r_3 \rightarrow -r_3$) and taking all r_i to infinity with $r_4 - r_3 > 0$ and finite reduces the diagram to the blowup of a \mathbf{Z}_3 orbifold. The flops $r_2 \rightarrow -r_2$ and $r_7 \rightarrow -r_7$ generate a $\mathbf{P}^1 \times \mathbf{P}^1$, and one can take external Kahler parameters to infinity to obtain this model. The equations for the $\mathbf{Z}_2 \times \mathbf{Z}_4$ singularity are $v^2 = yu$ and $v^4 = wzu^2$.



Diag. 7. Toric Diagram of $\mathbf{Z}_2 \times \mathbf{Z}_4$ Flopped Phase: $r_7 \rightarrow -r_7, r_4 - r_2 \rightarrow r_2 - r_4, r_3 \rightarrow -r_3$

Before solving the Picard-Fuchs equations, one must choose a basis that depends

both on the open as well as closed string phase. A priori there are many inequivalent basis choices, but in this model the requirement that the open string expansion converge in a particular phase limits the choices. Requiring the expansions in the z_i to converge in a neighborhood of the origin yields a unique solution for the particular phase. By uniqueness the solution solves the equations in any basis obtained from the original basis by a linear transformation in which the transformation matrix has no negative entries. The solution may not be unique in any particular basis. Also, even when the expansions are convergent in a particular basis, there may be a correction which is “nonperturbative” with respect to that basis and necessary for integrality. We have found a unique basis for this phase in which the above problem does not occur. We need to define $r_9 = r_6 - r_7$ for this basis. The solutions are as follows:

$$\begin{aligned}
z_1 &= \frac{q_1 e^{-N+T}}{1 + q_1 q_3} \\
z_2 &= q_2 (1 + q_1 q_3) e^{-N+M-T} \\
z_3 &= \frac{q_3 e^{N-T}}{1 + q_1 q_3} \\
z_7 &= q_7 (1 + q_2 q_3 q_9) e^{-P+M-T} \\
z_8 &= q_8 e^{N+P-2M} \\
z_9 &= \frac{q_9 e^{-M+2T}}{(1 + q_2 q_3 q_9)^2} \\
\Delta &= (t_1 + t_2 + 2t_7 + 2t_8 + t_9)^2 + \text{instanton corrections}
\end{aligned} \tag{3.2}$$

where Δ is a solution corresponding to a four-cycle,

$$T = \sum_{m,n,p,q,r,s} \frac{(-1)^{n+p+r+m} (n+m+p-r-2q-1)! z_1^r z_2^p z_3^m z_7^n z_8^s z_9^q}{m! q! r! (m-p-r+s)! (s-n)! (p-m-r)! (n-2q)! (p-2s+n-q)!},$$

$$N = \sum_{r,n,s} \frac{(-1)^s (2r-s-1)! z_1^r z_2^r z_7^{2n} z_8^s z_9^n}{n! r! (s-2n)! (r+n-2s)!},$$

$$M = \sum_{r,n,s} \frac{(-1)^{n+r} (2s-n-r-1)! z_1^r z_2^r z_7^{2n} z_8^s z_9^n}{r! n! (s-2r)! (s-2n)!},$$

and

$$P = \sum_{r,n,s} \frac{(-1)^s (2n-s-1)! z_1^r z_2^r z_7^{2n} z_8^s z_9^n}{n! r! (s-2r)! (r+n-2s)!}$$

and the z_i 's must be found as a function of the q_i 's perturbatively.

Examining Diagram (5) one sees that there is a reflection symmetry about a line through the equator of $\mathbf{P}^1(r_4)$ and $\mathbf{P}^1(r_8)$. The above solutions do not reflect this symmetry because any choice of basis necessarily breaks this symmetry. In this case the selection of q_3 breaks the symmetry. We had previously chosen the basis with q_6 instead of q_9 and found that the open string expansion did not give integers without the term $(1 + q_2q_3q_9) = (1 + q_2q_3q_6/q_7)$, but the perturbative solution, \hat{t}_6 , of the Picard-Fuchs equations does not converge if we include this term. The pieces of the solution involving negative powers solve the Picard-Fuchs equations by themselves so there are ambiguities of the solution in general. Clearly, the “nonperturbative” pieces are essential for integrality of the numerical invariants. We also note that this model is the only one treated so far where the above ambiguity involving negative powers occurs. In different phases of the theory we need to resolve the Picard-Fuchs equations.

Up to total order fourteen in the q_i 's (linear order in q_9) we find that the coefficients in the expansions of the inverse mirror map are integral. The expansions in this phase are $(z_1z_3 = \frac{q_1q_3}{(1+q_1q_3)^2})$

$$\begin{aligned}
z_1 &= q_1 + q_1q_2q_3 + q_1q_2q_3q_8 + q_1q_2q_7q_8 - 2q_1q_2q_3q_7q_8 + \cdots \\
z_2 &= q_2 + q_1q_2q_3 + q_2q_8 + q_1q_2q_3q_8 + \cdots \\
z_7 &= q_7 - q_2q_3q_7 + q_7q_8 + q_1q_2q_7q_8 - 2q_2q_3q_7q_8 + q_2q_3q_7q_9 + q_2q_3q_7q_8q_9 + \cdots \\
z_8 &= q_8 + q_1q_2q_8 + \cdots \\
z_9 &= q_9 - 2q_2q_3q_9 - q_8q_9 + q_1q_2q_8q_9 - 2q_2q_7q_8q_9 + 4q_2q_3q_7q_8q_9 - 2q_1q_2q_3q_7q_8q_9 + \cdots
\end{aligned} \tag{3.3}$$

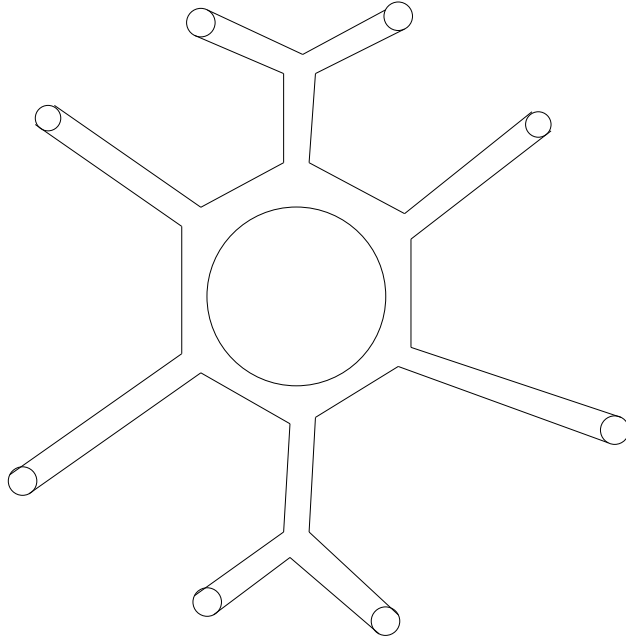
In the limit that $z_7 = z_8 = z_9 = 0$, $e^N = 1 + q_1q_2$, $e^T = 1 + q_2q_3$, and the solutions are precisely those of the $\mathbf{Z}_2 \times \mathbf{Z}_2$ case. The limit $z_1 = z_2 = z_3^{-1} = z_7 = z_8 = z_9 = 0$ while $z_2z_3z_7z_8$ is finite yields the solution for the blowup of the \mathbf{Z}_3 orbifold. Taking $z_1 = z_2^{-1} = z_3 = z_7^{-1} = z_8 = z_9 = 0$ with z_2z_3 and $z_2z_7z_8$ finite yields the $\mathbf{P}^1 \times \mathbf{P}^1$ case.

3.2. The Mirror and Open String Calculations

Putting $y_2 = u$, $y_6 = v$, and $y_7 = 0$ the equation for the mirror is

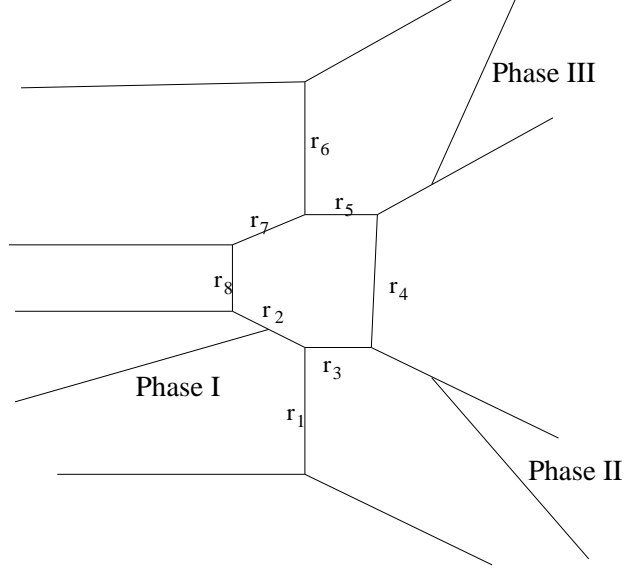
$$\begin{aligned}
xz = P(u, v) &= 1 + e^u + e^v + e^{u+v-t_1} + e^{u-v-t_2} + e^{v-u-t_3} + \\
&+ e^{-v-t_2-t_7-t_8} + e^{-2v+u-2t_2-t_8} + e^{-3v+u-3t_2-2t_7-2t_8-t_9} .
\end{aligned} \tag{3.4}$$

This choice is sensible for open string phases on the four-cycle. Notice again that this equation reproduces the $\mathbf{Z}_2 \times \mathbf{Z}_2$ case when $z_7 = z_8 = z_9 = 0$. To obtain the standard version of the \mathbf{Z}_3 case, take $v' = v - u - t_3$ and the previously discussed limit. The standard version of $\mathbf{P}^1 \times \mathbf{P}^1$ results from $u' = u - v - t_2$ and the above limit. The Riemann surface $P(u, v) = 0$ can be visualized in the following diagram.



Diag. 8. Riemann Surface $P(u, v) = 0$ in mirror of $\mathbf{Z}_2 \times \mathbf{Z}_4$ Blowup

A noncompact, supersymmetric three-cycle intersecting the toric base of the original manifold is determined by $|x_2|^2 - |x_7|^2 = c_1$, $|x_6|^2 - |x_7|^2 = c_2$, and $\sum_i \text{Arg}(x_i) = 0$. There are sixteen phases for the Lagrangian three-cycle with symmetries relating the phases in the lower half of diagram nine to those in the upper half. For instance the phase with a three-cycle intersecting $\mathbf{P}^1(r_7)$ is equivalent to phase I under the obvious permutation of the r_i 's and $v \rightarrow -v$. Also, phases II and III are equivalent. There are, accordingly, nine inequivalent phases.



Diag. 9. Phases for noncompact three-cycle in $\mathbf{Z}_2 \times \mathbf{Z}_4$ Blowup

Five of these phases can be parametrized by $u = 0$ after a change of coordinates while the rest correspond to $v = 0$. The latter yield quartic equations which can be solved and expanded, but the amount of computer time required seems prohibitively large. Fortunately, the $u = 0$ phases are quadratic. These are still quite complicated because the expansion involves seven variables. We will, thus, restrict ourselves to two of the u phases and only test the integer hypothesis at low order in the expansion. Phase I corresponds to $c_1 = 0$ and $0 < c_2 < r_2$. In phase II $c_1 = -r_3$ and $c_2 \ll 0$. In phase I we calculate the zero mode piece of u to be

$$\delta u = i\pi + \frac{t_1 - \hat{t}_1}{2} - \frac{t_3 - \hat{t}_3}{2} = i\pi - T + N. \quad (3.5)$$

We can determine δv by expanding an adjacent phase in which $u - v = 0$, and we find

$$\begin{aligned} \delta v &= i\pi + \frac{t_1 - \hat{t}_1}{4} - \frac{3(t_2 - \hat{t}_2)}{4} - \frac{t_7 - \hat{t}_7}{2} - \frac{t_8 - \hat{t}_8}{2} - \frac{t_9 - \hat{t}_9}{4} \\ &= i\pi - T + \ln(1 + q_1 q_3) \end{aligned} \quad (3.6)$$

Solving (3.4) for u and substituting instanton corrected variables, we can write the expan-

sion for \hat{u} in this phase.

$$\begin{aligned}
\hat{u} = & \sum'_{n,p,q,r} \left[\frac{(-1)^q (n-1)! e^{-Nn} e^{Mr} e^{Pq}}{p! q! r! (n-p-q-r)!} \times \right. \\
& e^{\hat{v}(4p+2r+q-3n)} q_1^p q_2^{3n-3p-2r-q} q_7^{2(n-p-r-q)} q_8^{2n-2p-2r-q} q_9^{n-p-r-q} \\
& - \sum'_{a,b,c,d,e,m,n,p} \left[\frac{(-1)^{b+d} (2n+m-1)!}{n! a! b! c! d! e! f! (n-a-b-c-d)! (p-f)! (m-p-e)!} e^{-T(2n+m)} e^{Mc} e^{Nb} e^{Pd} \times \right. \\
& (e^{\hat{v}(4a+3b+2c+d+m-2p-2n)} q_1^{a+e} q_2^{3n-3a-3b-2c-d+p+f} q_3^{n+e+f} \times \\
& \left. \left. q_7^{2(n-a-b-c-d)+p} q_8^{2n-2a-2b-2c-d+p} q_9^{n-a-b-c-d+f} \right) \right]
\end{aligned} \tag{3.7}$$

One can easily verify that the above expansion reduces to (2.13) in the limit $q_7 = q_8 = q_9 = 0$. Also, the limit $q_1 = q_9 = 0$ yields the \mathbf{F}_2 blown up at two points. One can also show that the inner phase of the \mathbf{Z}_3 model with ambiguity $n = 1$ is achieved in the limit $q_1 = q_2 = q_3^{-1} = q_7 = q_8 = q_9 = 0$ with $q_2 q_3 q_7 q_8$ finite and $\hat{v} \rightarrow \hat{v} + t_3$. In choosing this basis we have required that the expansion be convergent in a neighborhood of the origin in both open and closed string variables. In phase I this requirement entails that negative winding terms of the form $(\prod_i q_i^{n_i}) e^{-m\hat{v}}$ have $n_2 \geq m$. In an earlier calculation we chose a basis not meeting this last requirement and many terms had fractional invariants. Note that the basis with q_6 instead of q_9 does meet this latter requirement but still has fractions due to the nonperturbative piece. Up to linear order in q_9 , quadratic order in q_7 , cubic order in q_1 and q_3 , quartic order in q_2 and sixth order in $e^{\pm\hat{v}}$, all of the numerical invariants in this phase are integral. We present a table of terms corresponding to the homology classes that failed to be integral in the badly chosen basis.

3.3. Numerical Invariants

Table 4:

Numerical Invariants

k	m_1	m_2	m_3	m_7	m_8	m_9	$N_{k,\vec{m}}$	k	m_1	m_2	m_3	m_7	m_8	m_9	$N_{k,\vec{m}}$
2	1	3	2	2	2	1	-64	-2	1	3	0	2	2	1	0
2	0	4	2	2	2	1	-36	-2	2	4	0	2	2	1	0
2	0	4	2	2	3	1	-36	-2	0	3	1	2	2	1	1
3	0	3	3	2	2	1	-621	-2	0	4	2	2	2	1	4
3	1	4	3	2	2	1	-2214	-3	0	3	0	2	2	1	0
3	1	4	3	2	3	1	-2214	-3	1	4	0	2	2	1	0
3	3	3	3	2	2	1	72	-3	0	3	0	2	2	1	0
4	1	3	2	2	2	1	-128	-3	1	4	0	2	2	1	0
4	3	3	2	2	2	1	0	-4	0	4	0	2	2	1	0
4	0	4	2	2	2	1	-56	-4	0	6	2	4	4	1	0
4	0	4	2	2	3	1	-56	-4	0	6	2	4	5	1	0
6	1	3	2	2	2	1	-224	6	3	3	3	2	2	1	1026
6	3	3	2	2	2	1	0	6	1	4	3	2	2	1	-10656
6	0	4	2	2	2	1	-84	6	0	4	2	2	3	1	-84
6	0	3	3	2	3	1	-936	6	1	4	3	2	3	1	-10656

What is the meaning of these numerical invariants and why do we anticipate that the numerical invariants of this phase are integers? We consider the moduli space of maps from a Riemann surface of genus zero with one boundary into the Calabi-Yau such that the relative homology class of the image is labeled by the wrapping number on each two-sphere of the basis and the winding number around a noncontractible circle on the Lagrangian three-cycle. These maps should be holomorphic in the interior of the disk. The moduli space of these maps is generally noncompact, and one must add in extra maps that may be singular to define a compact space. There may be disconnected components of the moduli space when there are homotopically inequivalent maps into some relative homology class. One then defines a cohomology class analogous to the Euler class, and the numerical invariant is obtained by integrating this class over the moduli space. For the

case of genus zero closed strings, one should fix three complex parameters corresponding to $SL(2, \mathbf{C})$ transformations of the complex plane while for disks one fixes three real parameters corresponding to $SL(2, \mathbf{R})$ transformations of the upper half plane. If the dimension of the moduli space is zero after this fixing, the maps are isolated and the numerical invariants can be interpreted as counting curves. Otherwise, the integral over the moduli space could give fractions when there are orbifold singularities in the moduli space. Of course, there are many technicalities needed to make the above discussion rigorous.

A first principles calculation from the nonlinear sigma model point of view as described above is generally difficult. In this paper our determination of the invariants has been facilitated by an equivalent calculation on the local mirror. The drawback is that one does not have a direct argument that the invariants should be integers. Another approach is to start with the boundary linear sigma model that flows to the conformally invariant nonlinear sigma model at low energies. The relevant correlation functions that yield the numerical invariants are in a topological sector of the theory. The corresponding correlators in a topologically twisted version of the linear sigma model are scale invariant so the two calculations should be equivalent. The correlators are intersection forms on the moduli space of classical solutions with a given instanton number $m_i = \frac{1}{2\pi} \int_{\Sigma} F_i$ and winding number $k_p = \frac{1}{2\pi} \int_{\partial\Sigma} \Lambda_p$ where F_i is the gauge field strength which is integrated over the two-dimensional worldsheet Σ with boundary $\partial\Sigma$ and Λ_p is a boundary field which couples to the theta angle. It would be interesting to calculate correlators in the boundary linear sigma model corresponding to the numerical invariants. This correspondence between the two theories has been verified in several examples for closed worldsheets. Our aim here is to discuss the structure of the boundary linear sigma model moduli space in order to determine a criterion for integrality of the intersection forms. Assuming the correspondence is valid, we can apply this criterion to the nonlinear sigma model. Note that the moduli spaces of the two theories are different, but the correlators of this topological sector are expected to be the same.

In the linear sigma model the moduli space can be described as a space of holomorphic sections x_i of a line bundle over the upper half complex plane H of degree $d^i = \sum_j (m_j l_j^i + k_p l_p^{(1)i})$ (cf. (2.7)). One usually calls this bundle $\mathcal{O}(d^i)$. If $d^i \geq 0$, one can write a section as $x_i = \sum_{n=0}^{d^i} x_{in} z^n$ where z is a coordinate on H and the x_{in} must be chosen so that solutions of $x_i = 0$ all lie in H . If $d^i < 0$, there is no holomorphic section and $x_i = 0$. Note

that we have tried to indicate $\mathcal{O}(0)$ deformations of two-spheres on the toric diagram by drawing adjacent lines parallel. The moduli space takes the form

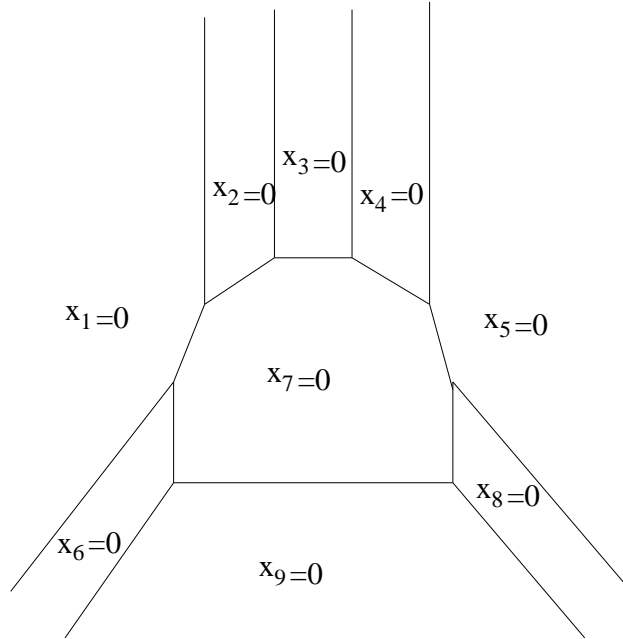
$$M_{\vec{m}, \vec{k}} = \frac{(X_{\vec{m}, \vec{k}} - I_{\vec{m}, \vec{k}})}{G} \quad (3.8)$$

where $X_{\vec{m}, \vec{k}}$ is the space of x_{in} such that x_i has zeroes in H . The maps x_i are singular whenever for some z , the values of x_i are “impossible”. We can readily see what is meant by “impossible” by examining Diagram (5). If we denote $D_i = \{(x_1, x_2, \dots, x_9) | x_i = 0\}$, then $I = \{(x_1, x_2, \dots, x_9) \in \cap_{l=1}^k D_l | \cap_{l=1}^k D_l \cap M = \phi\} \cup O$ where M is the toric manifold corresponding to Diagram (5). Then $I_{\vec{m}, \vec{k}}$ is the set of x_{in} such that for all z , $(x_1, x_2, \dots) \in I$. The moduli space is compactified by including maps where some points on the worldsheet are mapped into I . In general the moduli space could still be noncompact, but noncompact $\mathcal{O}(0)$ directions are generally cut off by the disk. For $\vec{k} = 0$, the moduli space is the Lagrangian three-cycle. Here O is determined by the disk constraints. For instance, in phase I of our case, $O = \{(x_1, x_2, \dots, x_9) | D_3 \cup D_6 \cup (D_7 \cap (M - D_2)) \cup (D_2 \cap (M - D_7))\}$. We mod out the set of allowed x_{in} by complex gauge transformations $G : x_{im} \rightarrow \prod_{j,p} (\alpha_j^{l_j^i} \beta_p^{l_p^{(1)i}} \gamma^{l^{(2)i}}) x_{im}$ where $\alpha_j \in \mathbf{C}^*$, $\beta_p \in \mathbf{R}^+$, and $\gamma \in U(1)$ (cf. (2.7)(2.8)). Writing $x_i = r_0(z - r_1) \dots (z - r_n)$, we see that this makes sense because we require $r_1, \dots, r_n \in H$ but $r_0 \in \mathbf{C}$ and $r_0 \neq 0$ if $x_i \neq 0$. The rescalings and rotations preserve the zeroes of x_i , and the condition $\sum_i \text{Arg}(x_i) = 0$ is redundant at the boundary of the disk on the toric base so $\gamma \equiv 1$ for disks stuck at the base. Note that all disks in the geometric phase are stuck at the base. We have shown that the moduli space is well defined. It is now easy to see that I includes any regions that are fixed by G unless we shrink some of the two-spheres to enter a nongeometric, orbifold phase. Since the moduli space of the geometric phase is smooth, the intersection form must give integers. On the other hand, the moduli space is frequently singular in nongeometric phases and fractions are possible. One may expect fractional terms when the boundary of the disk is fixed by the orbifold.

In phase II our coordinate transformation is $u \rightarrow u' = u - t_3$, $v \rightarrow v' = v$. We obtain $\delta u = i\pi + \frac{\delta t_1}{2} + \frac{\delta t_3}{2} = i\pi + \ln(1 + q_3)$ and δv as in (3.6). This phase reproduces precisely the outer phase (the three cycle intersects a noncompact two-cycle) of the \mathbf{Z}_3 case in the \mathbf{Z}_2 reflection of the limit discussed previously. This phase also reduces to the outer phase of the blown up \mathbf{F}_2 in the limit that $q_1 = q_9 = 0$. All of the corresponding terms are integral. In this phase $v' < 0$ and all terms have $k < 0$. Calculating to the same order as in phase I, we find that all terms are integral.

We have also calculated disk instantons in the nongeometric phase obtained by flopping $\mathbf{P}^1(r_6)$ and then flopping $\mathbf{P}^1(r_6 + r_7)$ at $x_4 = x_7 = 0$. In this phase $x_4 > 0$ so the flopped \mathbf{P}^1 is nongeometric. The calculation gives half-integer invariants for terms of the form $q_2^A q_3^2 q_8' e^{2n\hat{v}}$. ($r_8' = r_8 - r_2 + r_4 + r_6$, $n \in \mathbf{Z}^+$) These results are puzzling. Although there is a \mathbf{Z}_2 orbifold singularity on the “geometric” $\mathbf{P}^1(r_8')$ in this phase, the presence of the disk prevents the moduli space from being an orbifold. We believe the resolution of this paradox is that there is a “nonperturbative” contribution corresponding to P (3.2). The relative homology classes in question are present in Table 4. Depending on the choice of coordinates, one can have square root branch cuts ($\sqrt{q_8'}$) in the geometric phase but one can always find coordinates without branch cuts. The correction P is an expansion in the flopped Kahler parameter for which we need the analytic continuation to this phase. There are other terms in this phase in which the moduli space does contain orbifold singularities ($x_3 = x_5 = 0$, $x_2 \neq 0$), and we anticipate fractional invariants. We have not pursued this calculation further.

We have in this model a flop transition that augments the four-cycle from an \mathbf{F}^2 blown up at two points to one blown up at four points.



Diag. 10. Flopped Phase of $\mathbf{Z}_2 \times \mathbf{Z}_4$ Blowup: $r_1 \rightarrow -r_1$, $r_6 \rightarrow -r_6$

We can flop r_1 and r_6 to obtain this phase. The conifold type transitions occur for the part of the diagram that reduces to the $\mathbf{Z}_2 \times \mathbf{Z}_2$ case. As in that case one can substitute \mathbf{S}^3 's

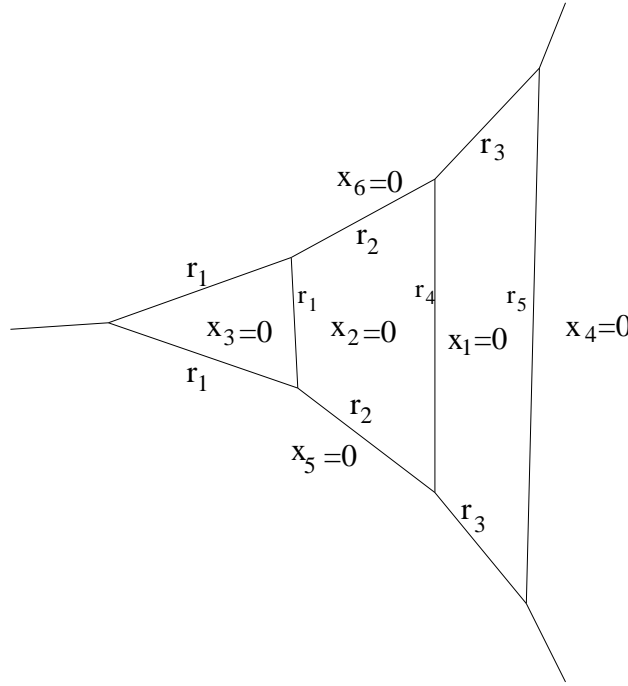
for \mathbf{P}^1 's. Our amplitudes $\mathcal{F}_{0,1}$ should correspond to Chern-Simons theory in a complicated background.

4. \mathbf{Z}_7

The \mathbf{Z}_7 case is interesting because there are three adjacent four-cycles. However, there are no geometric flops unlike the previous examples. The charges of six chiral fields under three $U(1)$'s are

$$\begin{aligned} l_1 &= (0, 1, -3, 0, 1, 1) \\ l_2 &= (1, -2, 1, 0, 0, 0) \\ l_3 &= (-2, 1, 0, 1, 0, 0). \end{aligned} \tag{4.1}$$

Solving the equations $\sum_j l_i^j |x_j|^2 = r_i$ generates the following toric diagram where $r_4 = r_1 + 3r_2$ and $r_5 = r_1 + 3r_2 + 5r_3$.



Diag. 11. Toric Diagram of \mathbf{Z}_7 Blowup

The instanton corrected Kahler parameters are given by

$$\begin{aligned} z_1 &= q_1 e^{-3M+P} \\ z_2 &= q_2 e^{M-2P+Q} \\ z_3 &= q_3 e^{-2Q+P} \end{aligned} \tag{4.2}$$

where

$$M = \sum_{n,m,p} \frac{(-1)^{n+m} (3n - m - 1)! z_1^n z_2^m z_3^p}{n!^2 p! (m - 2p)! (n - 2m + p)!},$$

$$P = \sum_{n,m,p} \frac{(-1)^{m+p} (2n - m - p - 1)! z_1^p z_2^n z_3^m}{p!^2 (n - 3p)! m! (n - 2m)!},$$

and

$$Q = \sum_{n,m,p} \frac{(-1)^m (2n - m - 1)! z_1^p z_2^m z_3^n}{n! p!^2 (m - 3p)! (n - 2m + p)!}.$$

These expressions for q_i must be inverted to obtain $z_i(q_i)$. The expansions are

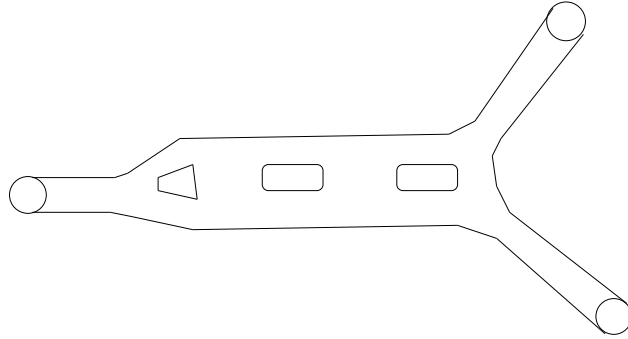
$$\begin{aligned} z_1 &= q_1 + 6q_1^2 + q_1 q_2 + 10q_1^2 q_2 + 4q_1^2 q_2^2 + q_1 q_2 q_3 + 10q_1^2 q_2 q_3 + 8q_1^2 q_2^2 q_3 + 4q_1^2 q_2^2 q_3^2 + \dots \\ z_2 &= q_2 - 2q_1 q_2 + 5q_1^2 q_2 - 2q_2^2 + 6q_1 q_2^2 - 20q_1^2 q_2^2 + q_2 q_3 - 2q_1 q_2 q_3 + 5q_1^2 q_2 q_3 \\ &\quad - 3q_2^2 q_3 + 8q_1 q_2^2 q_3 - 26q_1^2 q_2^2 q_3 - 2q_2^2 q_3^2 + 6q_1 q_2^2 q_3^2 - 20q_1^2 q_2^2 q_3^2 + \dots \\ z_3 &= q_3 + q_2 q_3 - 2q_1 q_2 q_3 + 5q_1^2 q_2 q_3 - 2q_1 q_2^2 q_3 - 2q_3^2 \\ &\quad - 3q_2 q_3^2 + 6q_1 q_2 q_3^2 - 15q_1^2 q_2 q_3^2 - 2q_2^2 q_3^2 + 12q_1 q_2^2 q_3^2 - 44q_1^2 q_2^2 q_3^2 + \dots \end{aligned} \tag{4.3}$$

There are also three more solutions to the Picard-Fuchs equations corresponding to four-cycles. The \mathbf{Z}_3 and \mathbf{Z}_5 cases can be obtained in the appropriate limit. To obtain \mathbf{Z}_3 we set $z_2 = z_3 = 0$.

The equation for the mirror can be written as

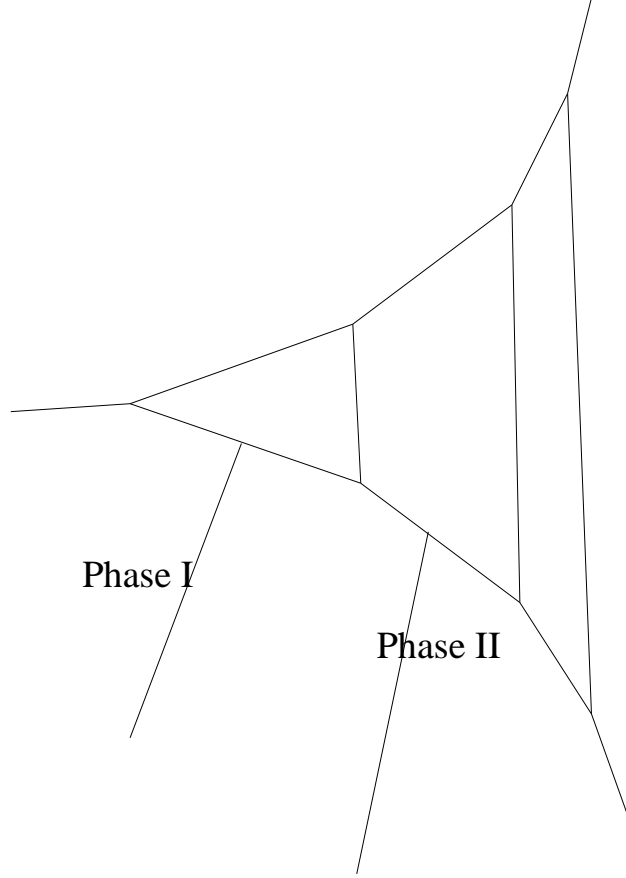
$$xz = P(u, v) = 1 + e^u + e^v + e^{-u-v-t_1} + e^{2u-t_2} + e^{3u-2t_2-t_3} \tag{4.4}$$

where $y_2 = u$, $y_5 = v$, and $y_3 = 0$. The Riemann surface that describes moduli of the three-cycle is a genus three surface with legs extending to infinity.



Diag. 12. Riemann Surface $P(u, v) = 0$ in mirror of \mathbf{Z}_7 Blowup

Clearly, we recover the $\mathcal{O}(-3) \rightarrow \mathbf{P}^2$ (\mathbf{Z}_3 blowup) when $z_2 = z_3 = 0$. Letting our Lagrangian three-cycle be determined by $|x_2|^2 - |x_3|^2 = c_1$, $|x_5|^2 - |x_3|^2 = c_2$, and $\sum_i \text{Arg}(x_i) = 0$; we find eight inequivalent phases taking into account the obviously symmetric phases.



Diag. 13. Phases for noncompact three-cycle in \mathbf{Z}_7 Blowup

Again some of the phases are described by quadratic equations, whereas others require a quartic equation. Phase I has $c_2 = 0$ and $c_1 \approx \frac{r_1}{2}$ while in phase II, $c_1 = c_2 \approx \frac{-r_2}{2}$. In phase I

$$\delta u = i\pi + \frac{1}{7}[-\delta t_1 + 4\delta t_2 + 2\delta t_3] = i\pi - M + P \quad (4.5)$$

and

$$\delta v = i\pi + \frac{1}{7}[-3\delta t_1 - 2\delta t_2 - \delta t_3] = i\pi - M. \quad (4.6)$$

In phase II δu is unchanged while $\delta v' = \delta v - \delta u = -P$. The results are shown in the tables.

Table 5:Phase I: $m_1 = 2, k = 3$

m_3	$m_2=0$	1	2	3	4
0	-9	-26	-49	-76	-110
1	0	-26	-76	-144	-232
2	0	0	-49	-144	-284
3	0	0	0	-76	-236
4	0	0	0	0	-118

Table 6:Phase I: $m_1 = 2, k = 4$

m_3	$m_2=0$	1	2	3	4
0	-12	-36	-72	-116	-172
1	0	-36	-112	-224	-372
2	0	0	-72	-224	-460
3	0	0	0	-116	-376
4	0	0	0	0	-180

Table 7:Phase I: $m_1 = 2, k = 5$

m_3	$m_2=0$	1	2	3	4
0	-15	-48	-99	-166	-250
1	0	-48	-156	-324	-552
2	0	0	-99	-324	-684
3	0	0	0	-166	-556
4	0	0	0	0	-258

Table 8:Phase I: $m_1 = 2, k = 6$

m_3	$m_2=0$	1	2	3	4
0	-19	-62	-132	-226	-349
1	0	-62	-208	-444	-772
2	0	0	-132	-444	-960
3	0	0	0	-226	-776
4	0	0	0	0	-355

Table 9:Phase II: $m_1 = 2, k = -3$

m_3	$m_2=0$	1	2	3	4
0	-3	-8	-19	-46	-110
1	0	-8	-28	-84	-232
2	0	0	-19	-84	-284
3	0	0	0	-46	-236
4	0	0	0	0	-118

Table 10:Phase II: $m_1 = 2, k = -4$

m_3	$m_2=0$	1	2	3	4
0	-4	-12	-32	-76	-172
1	0	-12	-48	-144	-372
2	0	0	-32	-144	-460
3	0	0	0	-76	-376
4	0	0	0	0	-180

Table 11:Phase II: $m_1 = 2, k = -5$

m_3	$m_2=0$	1	2	3	4
0	-5	-18	-49	-116	-250
1	0	-18	-76	-224	-552
2	0	0	-49	-224	-684
3	0	0	0	-116	-684
4	0	0	0	0	-258

Table 12:Phase II: $m_1 = 2, k = -6$

m_3	$m_2=0$	1	2	3	4
0	-7	-26	-36	-166	-347
1	0	-26	-112	-324	-772
2	0	0	-36	-324	-960
3	0	0	0	-166	-776
4	0	0	0	0	-355

There are nongeometric phases obtained by flopping the Kahler parameters. One would need to analytically continue the expansions (4.2) to calculate in these phases. The boundary conditions on the disk prevent the open instanton moduli space from being an orbifold even when the closed string instanton moduli space is an orbifold unless the boundary of the disk is fixed by the orbifold. In this case fractional invariants are possible.

Acknowledgments

I wish to acknowledge J. Distler and A. Iqbal for beneficial discussions and R. McNees for answering Mathematica related questions. This work was supported in part by NSF grant PHY-0071512.

References

- [1] M. Aganagic, A. Klemm, and C. Vafa, hep-th/0105045.
- [2] D. Morrison and M. Plesser, Nucl. Phys. **B440** (1995), hep-th/9412236.